

An assessment of the on-orbit performance of the CALIPSO Wide Field Camera

Michael C. Pitts*, Larry W. Thomason, Yongxiang Hu, David M. Winker
NASA Langley Research Center, 23A Langley Boulevard, Hampton, VA, USA 23681

ABSTRACT

The Wide Field Camera (WFC) is one of three instruments in the CALIPSO science payload, with the other two being the Cloud-Aerosol Lidar with Orthogonal Polarization (CALIOP) and the Infrared Imaging Radiometer (IIR). The WFC is a narrow-band, push-broom imager that provides continuous high-spatial-resolution imagery during the daylight segments of the orbit over a swath centered on the CALIOP footprint. The instantaneous field of view of each WFC pixel is approximately 125 m x 125 m when projected on the Earth's surface from an orbit altitude of 705 km. The spectral band of the WFC, with a center wavelength of 645 nm and a FWHM bandwidth of 50 nm, is designed to match the Aqua MODIS instrument's channel 1. The primary WFC Level 1 products are radiance and reflectance registered to an Earth-based grid centered on the CALIOP ground track. "First light" WFC images were acquired on 18 May 2006 and routine data acquisition began in early June 2006. An initial science assessment of the WFC on-orbit performance was conducted based on analysis of the first twelve months of flight data. Comparisons of the WFC measurements with the well-calibrated Aqua MODIS channel 1 data were performed to evaluate the on-orbit radiometric performance of the WFC. Overall agreement is excellent, especially over bright deep convective clouds where the WFC measurements agree to within a few percent of MODIS. This paper provides a summary of our overall assessment of the on-orbit radiometric performance of the WFC.

Keywords: CALIPSO, WFC, imager

1. INTRODUCTION

Clouds and aerosols play an important role in the Earth's climate system. Their role is complex, however, and there are large uncertainties in the impact of clouds and aerosols on the Earth's radiation budget. These uncertainties limit our understanding of the climate system and the potential for global climate change. The Cloud-Aerosol Lidar and Infrared Pathfinder Satellite Observations (CALIPSO) mission is designed to provide global, vertically resolved measurements of clouds and aerosols that will complement current measurements and improve our understanding of their role in climate forcing^{1,2}. Launched on 28 April 2006, CALIPSO is part of the Aqua satellite constellation (or A-train) that consists of the Aqua³, CloudSat⁴, CALIPSO, PARASOL⁵, and Aura⁶ satellite missions. All of the A-train satellites are in a 705-km sun-synchronous orbit with approximately a 1:30 pm equatorial crossing and a 16-day repeat cycle. The orbit inclination of 98.2° provides nearly global measurement coverage between 82° N and 82° S. The CALIPSO satellite flies behind the Aqua satellite with an along-track separation of less than 2 minutes. The CALIPSO orbit is slightly inclined to that of Aqua so that CALIPSO is located 215 km east of Aqua when crossing the Equator on the day side of the orbit. This inclination insures the CALIPSO footprint remains outside the sunglint pattern observed by the Aqua MODIS instrument.

The CALIPSO science payload consists of three co-aligned nadir viewing instruments: the Cloud-Aerosol Lidar with Orthogonal Polarization (CALIOP), the Infrared Imaging Radiometer (IIR), and the Wide Field Camera (WFC). CALIOP is a dual-wavelength, polarization sensitive lidar that provides high vertical resolution profiles of cloud and aerosol properties. The IIR, developed by the French space agency CNES, provides calibrated radiances at 8.7 μm , 10.6 μm , and 12 μm over a 64-km swath. The WFC, developed by Ball Aerospace, is a narrow-band push-broom imager that provides continuous high spatial resolution (125-m) images of radiance and reflectance during the daylight segments of the orbit over a 61-km swath centered on the lidar footprint. The spectral band of the WFC is designed to match the Aqua MODIS instrument's channel 1 having a central wavelength of 645 nm and a bandwidth of 50 nm.

* Michael.C.Pitts@nasa.gov

One of the primary uses of the WFC is to accurately co-register the CALIPSO lidar data with data from MODIS and other instruments on the A-Train constellation to facilitate joint CALIPSO/A-Train retrievals. Another important role of the WFC is to provide supplemental data to the CALIPSO IIR retrievals of cloud microphysical properties. For instance, the visible wavelength WFC radiometric data will be utilized to identify the presence of low cloud and assess homogeneity over the IIR footprint. Additional applications of the WFC data will be to provide overall meteorological context to CALIPSO imagery and to verify the pointing accuracy of the CALIPSO platform.

Accurate knowledge of the WFC pointing and the radiometric accuracy are critical to the science applications described above. Therefore, one of our first priorities after launch was to assess the overall performance of the WFC on orbit. In this paper, we present results from this initial assessment.

2. WIDE FIELD CAMERA DESCRIPTION

The WFC is a commercial-off-the-shelf instrument based on the Ball Aerospace & Technologies Corporation CT-633 star tracker design. Although the WFC is designed with a 512 x 512 CCD array, it essentially operates as a push broom line camera by reading out only one row of pixels per image frame. To minimize spatial smearing during the CCD readout operations, most of the CCD is masked off except for approximately 30 rows near the center. If necessary, the target row for readout can be reprogrammed on orbit. The WFC image plane is oriented such that the target row of pixels is aligned in the cross track direction. The instantaneous field of view of each pixel is approximately 125 m x 125 m when projected onto the Earth's surface from an orbit altitude of 705 km. Nominally, 488 of the 512 pixels in the target row are utilized providing a full swath field of view of 61 km in the cross-track direction, centered on the lidar telescope boresight. A summary of the WFC performance specifications is provided in Table 1.

Due to downlink data rate limitations, the WFC data is not retained at full 125-m resolution across the entire image. Pixels outside the central 5-km of the cross-track swath are averaged on-board in both the cross-track and along-track directions to produce low resolution (1 km x 1 km) image samples. The resultant downlinked WFC images consist of two low-resolution swaths (each 28-km wide) on either side of a high resolution swath (5-km wide) centered on the lidar ground track. The WFC swath is illustrated schematically in Figure 1a. An example of a downlinked WFC Level 0

Table 1. Wide Field Camera specifications.

Parameter	Specification	Comment
Spectral Band	620-670 nm	Matched to Aqua MODIS Channel 1
Single pixel IFOV	125 m x 125 m at Earth's surface	24 μm pixels 135-mm focal length
Full Swath FOV	61 km	488 pixels cross-track
Dynamic Range	16 bits	Standard on CT-633
SNR at L_{max} ($730 \text{ Wm}^{-2}\mu\text{m}^{-1}\text{sr}^{-1}$)	435	f/8 lens and full-well capacity of 150 ke^-
SNR at L_{typ} ($12 \text{ Wm}^{-2}\mu\text{m}^{-1}\text{sr}^{-1}$)	51	As above
Radiometric Response Stability	< 1% over 24 hours	Temperature stabilized with TEC

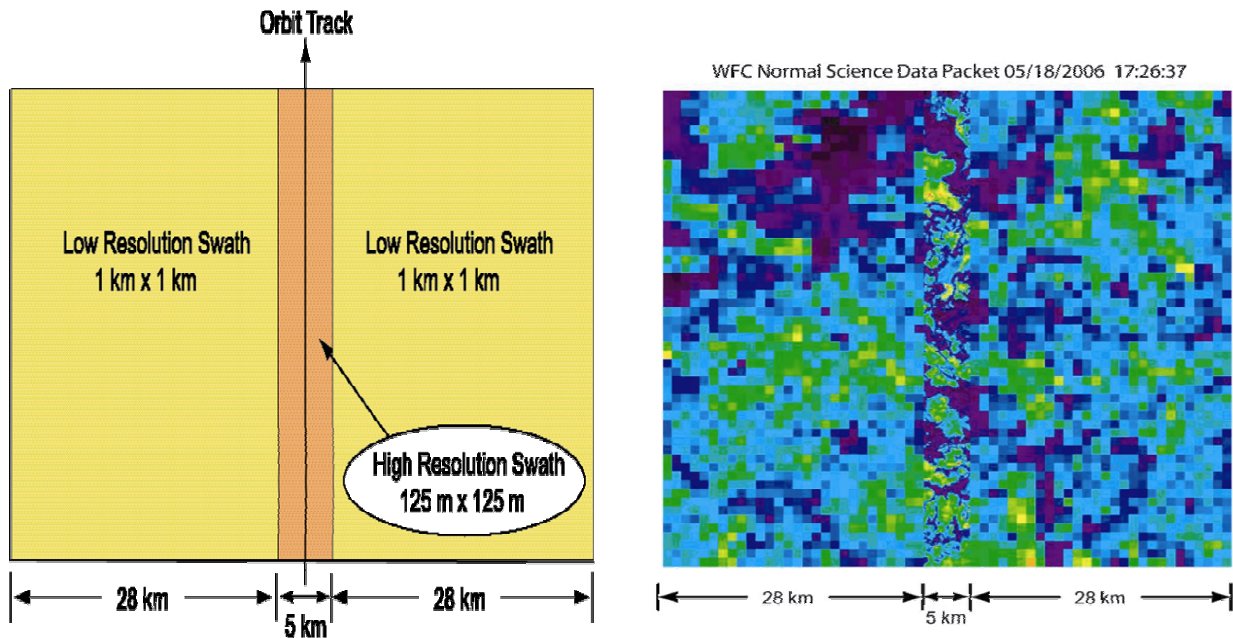


Fig. 1. The WFC swath is illustrated schematically in the left hand panel. Due to downlink data rate limitations, data outside the central 5-km of the swath are averaged on-orbit to 1-km x 1-km resolution. An example of a downlinked WFC Level 0 data packet is shown in the right hand panel. The low resolution (1-km) and high resolution (125-m) swaths are visible in the Level 0 data packet.

Science Data Packet is shown in Figure 1b. The two low resolution swaths and central high resolution swath are clearly visible in the Level 0 Science Data packet.

The primary WFC Level 1 science data products are calibrated radiance and bi-directional reflectance, registered to an Earth-based grid centered on the lidar ground track. For each orbit, three different data grids are produced. The 125-m x 125-m Native Science grid contains only the central 5-km wide high resolution portion of the WFC swath. The 1-km x 1-km Native Science grid contains the full 61-km wide swath. The 1-km x 1-km Registered Science grid provides WFC data on the identical grid as the CALIPSO IIR data and is produced to facilitate the use of the WFC data in the IIR retrievals. In addition to radiance and reflectance grids, the WFC Level 1 data products include two parameters to quantify the homogeneity of the cross-track image frames: swath homogeneity and track homogeneity. For more information on the WFC Level 1 Science Data Sets and how to access the data please visit www-calipso.larc.nasa.gov.

3. ON-ORBIT PERFORMANCE ASSESSMENT

The WFC is designed to have a large dynamic range that will allow it to observe bright clouds without saturation and still be able to resolve small variations in surface albedo for geolocation assessment applications. To achieve its science objectives, the WFC must also exhibit good radiometric stability. To monitor the radiometric stability and characterize long-term trends, a number of vicarious calibration activities have been performed. "First light" WFC images were acquired on 18 May 2006 and routine data acquisition began in mid-June 2006. A detailed assessment of the on-orbit performance of the WFC has been performed based on flight data from the first twelve months of the mission. This assessment included analyses of both the radiometric performance and pointing accuracy of the WFC. Although this report will focus on the radiometric performance of the WFC, a brief summary of the results of the pointing verifications is provided below.

3.1 Geolocation Assessment

The WFC pointing and geolocation verification was performed utilizing a coastline detection algorithm⁷. Small offsets in the WFC pointing were identified. These offsets have been corrected as part of the Level 1 data processing. The

uncertainty in the geolocation is now estimated to be less than 100 m. In addition, the lidar and WFC co-alignment was verified through correlation analyses of lidar and WFC reflectance measurements with the lidar footprint falling within the center pixel of the WFC swath.

3.2 Radiometric Calibration

There is no on-orbit calibration capability for the WFC. Therefore we must rely on vicarious approaches to verify and monitor the WFC radiometric calibration. Since the WFC bandpass is matched to the well-calibrated Aqua MODIS Channel 1, direct comparisons with nearly coincident MODIS Channel 1 measurements provide an excellent means of assessing the WFC radiometric performance. Figure 2 shows an example of a WFC radiance image and the Aqua MODIS Channel 1 radiance image for the 200-km wide portion of the MODIS swath centered on the CALIPSO ground track. Qualitatively, the WFC and MODIS images are in good agreement. A more quantitative comparison is achieved by comparing the observed distribution of reflectance from the two instruments. Figure 3 shows preliminary comparisons of WFC and MODIS reflectance distributions for a single day of observations. The initial WFC V1.01 data based on pre-launch instrument calibration (blue curve in Figure 3) was systematically biased about 10% high relative to MODIS data. Further investigation revealed that this bias was caused by a previously uncharacterized offset in the reported WFC exposure time. On-orbit diagnostic experiments indicated that the actual exposure time is approximately 0.4 ms longer than is actually reported (3.4 ms versus 3.0 ms) which produces a high bias in the derived radiometric data. This offset has been corrected in the WFC V1.10 data that was released to the public in December 2006 (black curve in Figure 3). As Figure 3 illustrates, the WFC V1.10 data are now much closer in magnitude to the MODIS data.

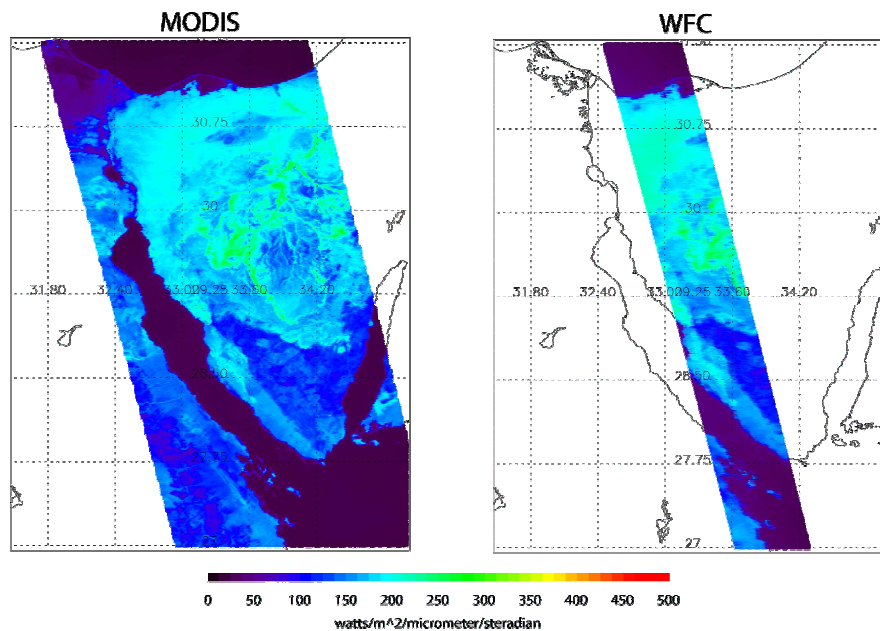


Fig. 2. This figure shows examples of Aqua MODIS (left panel) and WFC (right panel) radiance images. The MODIS image shown is a 200-km wide portion of the full MODIS swath centered on the CALIPSO ground track.

Due to the slight inclination of the CALIPSO orbit relative to Aqua, the WFC swath falls in the right side of the full MODIS swath, with the center of the WFC swath located about 215 km east of the center of the MODIS swath as the satellites cross the Equator on the day side of the orbit. As a result, there are significant viewing geometry differences between the WFC and MODIS observations. All WFC measurements are within a few degrees of nadir. However, the subset of MODIS pixels coincident with the WFC swath have viewing angles as large as 20 degrees. Such large differences in viewing geometry can introduce large differences in the observed reflectance, depending on the angular scattering properties of the underlying scene. To minimize the effects of these viewing geometry differences, we will utilize deep convective clouds as vicarious calibration targets. Analysis of data from the CERES experiment has shown that cold (i.e. optically thick with brightness temperatures < 205 K) tropical convective clouds possess uniform and

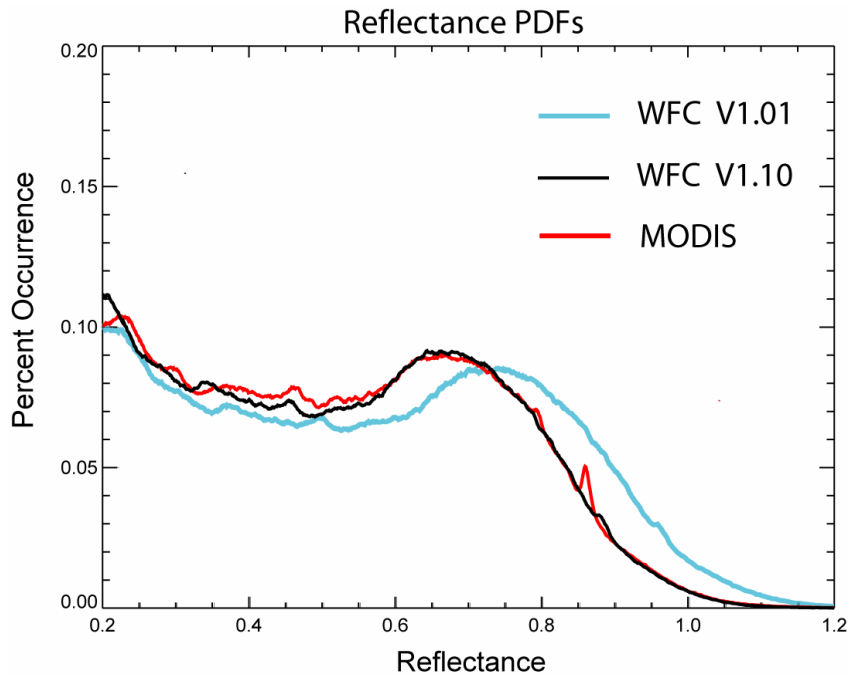


Fig. 3. This figure shows comparisons of WFC and MODIS reflectance distributions for a single day. The preliminary WFC V1.01 data is represented by the blue line. The public released WFC V1.10 data is indicated by the black line. MODIS data is indicated by the red line.

stable reflectance properties that allow them to be used as shortwave calibration targets⁸. There are numerous advantages to using these clouds as vicarious calibration targets. First of all, convective clouds with tops higher than 12 km are encountered frequently in the tropics so it is possible to obtain a sufficient number of samples to produce robust statistics over periods of one month or less. For optical depths greater than a few hundred, cloud albedo becomes independent of the cloud optical depth. Moreover, when viewed from above, these clouds are very bright and the albedo and angular scattering characteristics of these clouds are very uniform and stable from month to month. Furthermore, the reflectance is spectrally uniform. Additionally, due to their large vertical extent (cloud top heights > 12 km), aerosol and water vapor concentrations above these clouds are small and the atmospheric transmittance from satellite to cloud top can be estimated with high accuracy. Therefore, these clouds represent the most stable, standard targets to monitor the end-to-end radiometric calibration of the WFC.

In these analyses, we use a simple set of criteria to identify deep convective scenes in the WFC and MODIS data. First, the mean radiance of the scene must exceed a threshold of $400 \text{ Wm}^{-2}\text{sr}^{-1}\mu\text{m}^{-1}$. In addition, to restrict our comparisons to relatively uniform scenes, we require the cross-track variance of the scene to be less than 7.5%. Based on these criteria, we searched the WFC and Aqua MODIS Channel 1 data and identified all coincident deep convective cloud observations during approximately the first year of the CALIPSO mission. Reflectance and radiance statistics were then compiled from these deep convective cloud databases on either a daily or monthly basis. A comparison of WFC/MODIS radiance observations over these deep convection scenes for a series of days (about 1 day per week) throughout the first 12 months of the CALIPSO mission is shown in Figure 4. This scatter plot illustrates the compact relationship between the two data sets. A time series of the mean MODIS-WFC radiance differences for each of the series of days is shown in the Figure 5. Although the WFC radiances appear biased slightly low relative to MODIS, the WFC data tracks the MODIS data very closely over the entire time period with the largest differences never exceeding about 1.2%.

Comparisons of the monthly distributions of deep convective cloud reflectance provide more insight to the stability of the WFC calibration relative to MODIS. Distributions for four different months are shown in Figure 6. Although the overall shape of the distributions changes slightly from month to month, the WFC reflectance distributions are in excellent agreement with the MODIS distributions for all the months. The peak WFC reflectance values for each

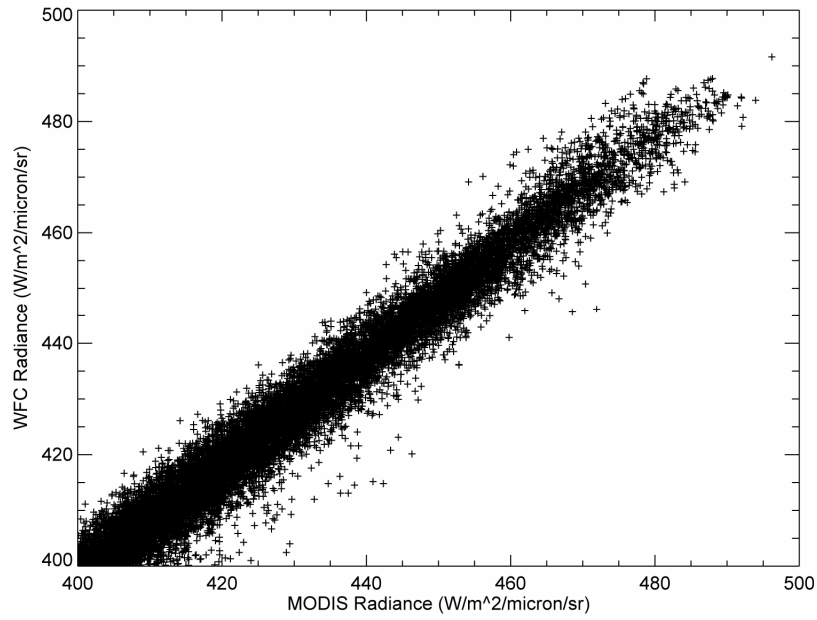


Fig. 4. This figure shows a scatter plot of WFC and MODIS radiances over deep convective clouds for a series of days during the first 12 months of the CALIPSO Mission.

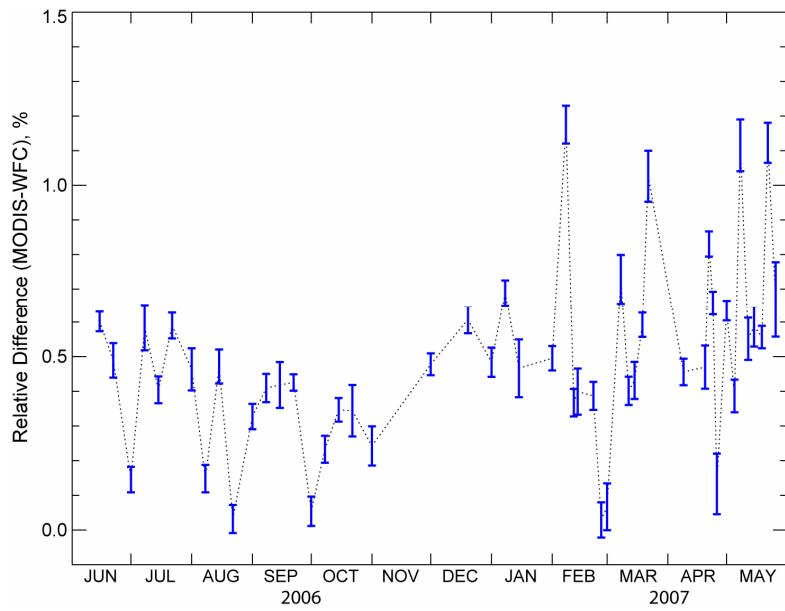


Fig. 5. This figure shows a time series of differences between WFC and MODIS daily mean radiances over deep convective clouds. The error bars represent one standard deviation from the mean.

individual month are always within a few percent of the MODIS values. These comparisons illustrate that the WFC radiometric calibration has remained stable to within a 1-2% with no apparent drift relative to MODIS during the first 12 months of operation.

We also examined the month-to-month variations in the WFC deep convective cloud distributions alone to determine if any calibration drift is detectable. The distributions from five different months are shown in Figure 7. The variance of the low reflectance tail is likely due to the inclusion of some thinner clouds in some months. The measurements in the high reflectance tail are from the brightest and most uniform clouds and the variance in this portion of the distribution is very small, indicating that the WFC has been very stable over the first 12 months. The peak reflectance from month-to-month varies by less than a few percent. Overall, these comparisons provide confidence that the WFC has exhibited excellent stability over the first year of operation.

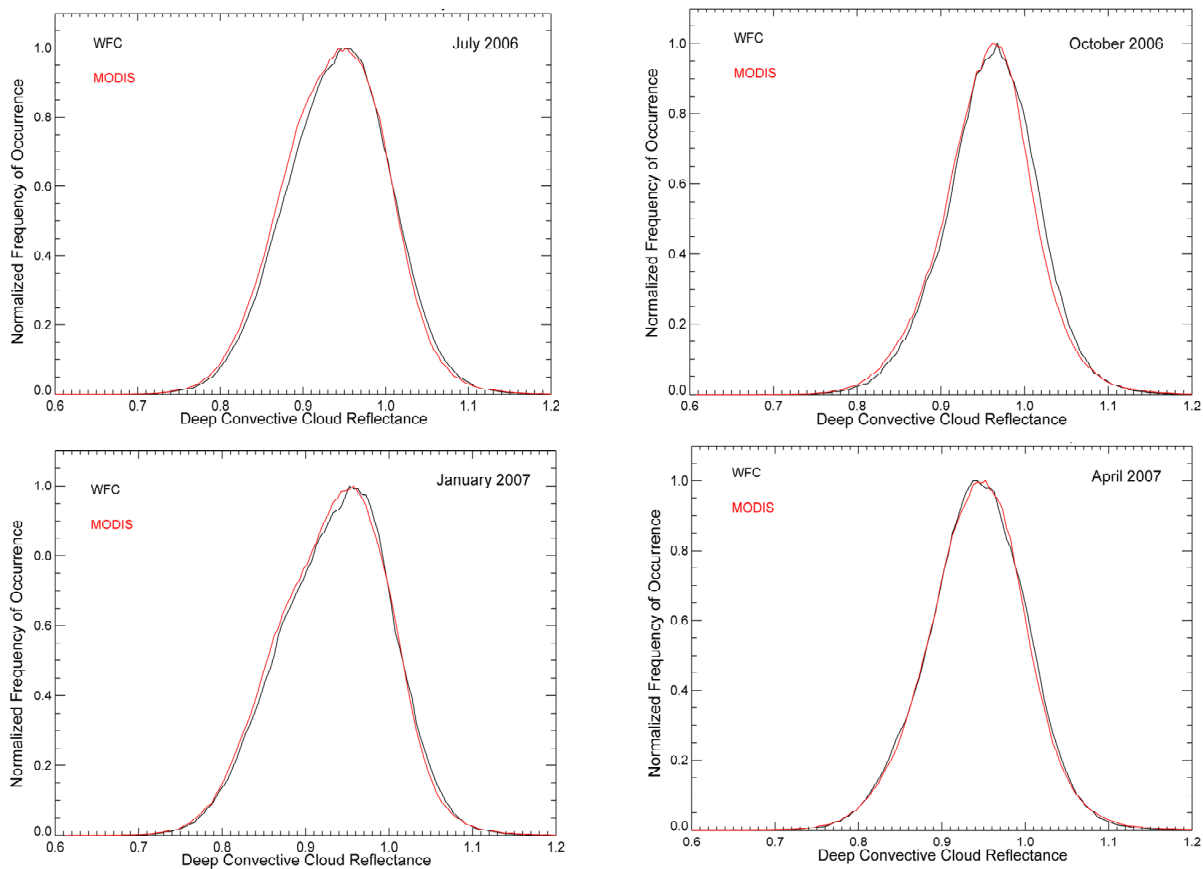


Fig. 6. This figure shows comparisons of monthly distributions of deep convective cloud reflectance from the WFC (black lines) and MODIS (red lines) for four different months.

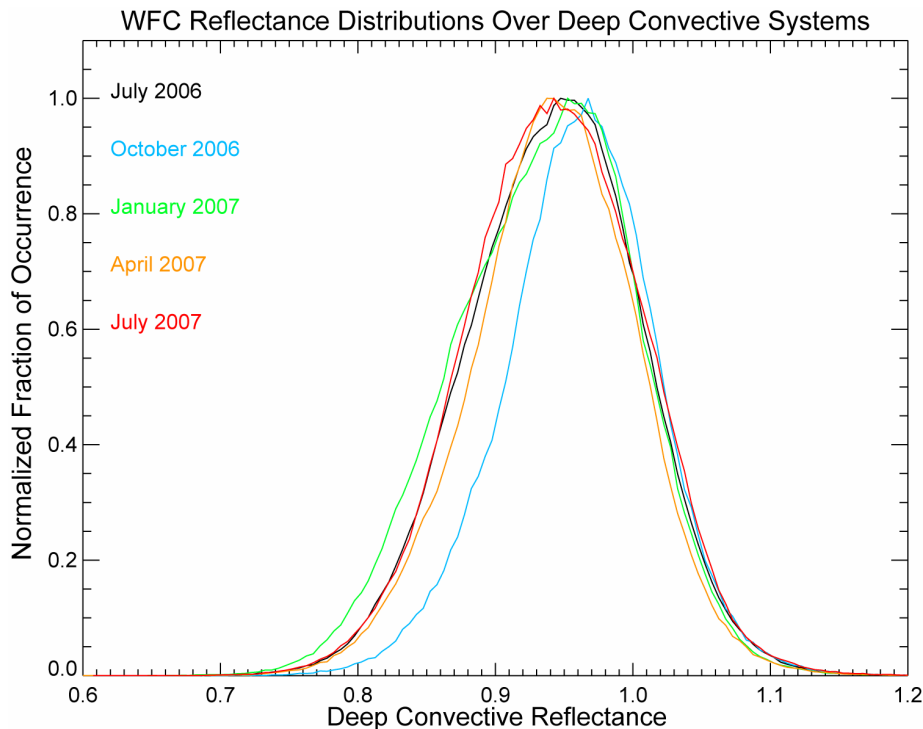


Fig. 7. This figure shows the distribution of WFC reflectance from deep convective clouds from five different months as indicated in the figure.

4. SUMMARY

In this paper, we have provided an assessment of the radiometric performance of the CALIPSO WFC during its first year of operation. Using deep convective clouds as vicarious calibration targets, direct comparisons of nearly coincident WFC and MODIS radiance measurements showed that the WFC radiance tracks the MODIS data very closely with daily mean differences never exceeding 1.2%. Analyses of WFC and MODIS monthly deep convective cloud reflectance distributions also indicate that the WFC has exhibited excellent radiometric stability during the first year of operation with no apparent drift relative to MODIS.

REFERENCES

- ¹ D. M. Winker, J. Pelon, and M. P. McCormick, "The CALIPSO mission: Spaceborne lidar for observation of aerosols and clouds," in *Lidar Remote Sensing for Industry and Environmental Monitoring III, Proc. SPIE vol. 4893*, edited by U. N. Singh, T. Itabe, and Z. Lui, pp. 1-11, SPIE, Bellingham, WA, 2003.
- ² D. Winker, B. Hunt, and M. McGill, "Initial performance assessment of CALIOP," *Geophys. Res. Lett.*, *34*, L19803, doi:10.1029/2007/GL30135, 2007.
- ³ C. L. Parkinson, "Aqua: An Earth-observing satellite mission to examine water and other climate variables," *IEEE Transactions on Geoscience and Remote Sensing*, *41*, 173-183 (2003).
- ⁴ G. L. Stephens, D. G. Vane, R. J. Boain, G. G. Mace, K. Sassen, Z. Wang, A. J. Illingworth, E. J. O'Connor, W. B. Rossow, S. L. Durden, S. D. Miller, R. T. Austin, A. Benedetti, C. Mitrescu, and the CloudSat Science Team, "The

CloudSat mission and the A-Train: A new dimension of space-based observations of cloud and precipitation,” *Bulletin of the American Meteorological Society*, **83**, 1771-1790 (2002).

⁵ F. Steinmetz, D. Ramon, P.-Y. Deschamps, and J.-M. Nicolas, “Analysis of the first ocean color products from POLDER 3 onboard PARASOL,” in *Remote Sensing of the Ocean, Sea Ice and Large Water Regions 2005*, Proceedings of the SPIE Vol. 5977, edited by C. R. Bostater, R. Santoleri, pp. 1-9, SPIE, Bellingham, WA, 2005.

⁶ M. R. Schoeberl, A. R. Douglass, E. Hilsenrath, P. K. Bhartia, R. Beer, J. W. Waters, M. R. Gunson, L. Froidevaux, J. C. Gille, J. J. Barnett, P. E. Levelt, and P. DeCola, “Overview of the EOS Aura Mission,” *IEEE Transactions on Geoscience and Remote Sensing*, **44**, 1066-1074 (2006).

⁷ C. Currey, Geolocation Assessment Algorithm for CALIPSO Using Coastline Detection, *NASA Technical Paper 2002-211956*, 2002.

⁸ Y. Hu, B. A. Wielicki, P. Yang, P. W. Stackhouse, B. Lin, and D. F. Young, Application of Deep Convective Cloud Albedo Observation to Satellite-Based Study of the Terrestrial Atmosphere: Monitoring the Stability of Spaceborne Measurements and Assessing Absorption Anomaly, *IEEE Transactions on Geoscience and Remote Sensing*, **42**, 2004.